

RESEARCH

Open Access



The intra-tumoral microbiome as a potential biomarker of response to external beam radiation therapy in cervical cancer

Zhongyan Dou^{1†}, Conghui Ai^{2†}, Jinping Zhang^{3†}, Kangming Li¹, Meiping Jiang¹, Xingrao Wu¹, Chunfang Zhao¹, Zheng Li^{4*} and Lan Zhang^{1*}

Abstract

Background We aimed to determine the potential predictive value of the intra-tumoral microbiome as a marker of the response to external beam radiation therapy (EBRT) in cervical cancer (CC).

Methods A prospective longitudinal trial of 36 CC patients receiving pelvic radiotherapy was designed to investigate microbial characteristic signatures and diversity (alpha and beta) of multiple sites (tumor, vaginal, gut, urethral, and oral) in the superior response (SR) and inferior response (IR) groups of CC patients by 16S rRNA sequencing. Utilized the least absolute shrinkage and selection operator (LASSO) logistic regression method to analyze clinicopathological factors that potentially influenced the efficacy of EBRT. LEfSe analysis highlighted the microbiome features that best distinguished the categorized patient samples. Selected parameters were validated with Spearman correlation analysis, receiver operating characteristic (ROC) area under the curve (AUC) analysis and Kaplan-Meier survival analysis.

Results Firstly, in our cohort, LASSO logistic regression analysis revealed no association between clinicopathological factors and EBRT efficacy. Subsequently, we employed 16S rRNA sequencing to compare microbiome differences across multiple sites and their correlations with major clinicopathological factors. We discovered that the intra-tumoral microbiome was independent of clinicopathologic features and represented the most direct and reliable reflection of the microbial differences between the SR and IR groups. We found lower alpha diversity in the tumor microbiome of SR group and identified the most relevant microbiome taxa (*Bifidobacteriaceae*, *Beijerinckiaceae*, and *Orbaceae*) associated with the efficacy of the response to EBRT in CC patients. We then conducted ROC analysis, finding that specific microbial taxa had an AUC of 0.831 (95% CI, 0.667–0.995), indicating the potential of these taxa as biomarkers for predicting EBRT efficacy. Kaplan-Meier survival analysis showed a better prognosis for patients with lower alpha diversity and higher relative abundance of *Bifidobacteriaceae*.

[†]Zhongyan Dou, Conghui Ai and Jinping Zhang contributed equally to this work.

*Correspondence:
Zheng Li
lizheng@kmmu.edu.cn
Lan Zhang
zhanglan@kmmu.edu.cn

Full list of author information is available at the end of the article



© The Author(s) 2024. **Open Access** This article is licensed under a Creative Commons Attribution-NonCommercial-NoDerivatives 4.0 International License, which permits any non-commercial use, sharing, distribution and reproduction in any medium or format, as long as you give appropriate credit to the original author(s) and the source, provide a link to the Creative Commons licence, and indicate if you modified the licensed material. You do not have permission under this licence to share adapted material derived from this article or parts of it. The images or other third party material in this article are included in the article's Creative Commons licence, unless indicated otherwise in a credit line to the material. If material is not included in the article's Creative Commons licence and your intended use is not permitted by statutory regulation or exceeds the permitted use, you will need to obtain permission directly from the copyright holder. To view a copy of this licence, visit <http://creativecommons.org/licenses/by-nc-nd/4.0/>.

Conclusions Our data suggested that intra-tumoral specific microbiome taxa and lower alpha diversity may play an important role in the CC patient sensitivity to EBRT and offer novel potential biomarkers for predicting the response to EBRT efficacy.

Keywords Cervical cancer, Diversity, External beam radiation therapy, Intra-tumoral microbiome, Potential biomarker

Introduction

Cervical cancer (CC), a common female reproductive system malignancy, is the fourth leading cancer in terms of global incidence and mortality rates among women [1]. The main treatment for CC involves surgical resection and radiotherapy [2]. In accordance with the International Federation of Gynecology and Obstetrics (FIGO) staging system, radiotherapy is equally effective as surgery for early cervical cancer, and radical radiotherapy and chemotherapy can be considered for advanced cases [3]. External beam radiation therapy (EBRT) and brachytherapy are the forms of radiotherapy used for CC. The tumor volume reduction rate (TVRR) post-EBRT of CC represents an essential indicator of sensitivity to radiotherapy and a predictor of prognosis. Some patients are insensitive or resistant to radiotherapy, resulting in poor treatment efficacy, recurrence, or metastasis, which remains a significant hurdle to CC therapeutics [4, 5]. Therefore, exploring potential targets to overcome radiation-resistance is crucial for improving treatment outcomes.

The human microbiome refers to the genome of microorganisms (bacteria, archaea, fungi, and viruses) that live in different body parts and are responsible for more than 98% of the genetic activity of the human body [6]. The intra-tumoral microbiome represents the genome of microorganisms present in the tumor parenchyma and the microenvironment surrounding the tumor [6]. It has been demonstrated that the intra-tumoral microbiome that exists in the majority of solid tumors are mostly intra-cellular and present in both cancer and immune cells [7, 8]. The microbiome plays an important role in regulating multiple biological processes such as modulation of cancer susceptibility [9], promotion of cancer cell metastasis [8], and immune modulation [10]. The microbiome has been shown to be remarkably associated with radiosensitivity in malignant tumors and is participating in the regulation of radiosensitivity in hepatocellular carcinoma [11], esophageal squamous cell carcinoma [12], colorectal cancer [13] and other tumors. However, the specific mechanism underlying this association between the microbiome and radiosensitivity is not yet clear. Previous researches on the cervical microbiome have focused primarily on the impact of the intra-vaginal microbiome on the pathogenesis of CC, rarely exploring the role of the intra-tumoral microbiome in tumor development and prognosis [14, 15]. Understanding the diverse contributions of the bacterial microbiota to

cancer treatment is vitally important for determining the prognosis of CC.

In this study, we explored intra-tumoral microbiome diversity and specific microbiome taxa in relation to EBRT. We performed next-generation sequencing of 16S rRNA to investigate microbial characteristics at multiple sites in CC patients divided into superior response (SR) and inferior response (IR) groups and evaluated the efficacy of EBRT using TVRR=66.7% as the optimal cut-off value according to a previous study [16]. Developing specific intra-tumoral microbiomes as potential biomarkers may improve the therapeutic outcomes of radiotherapy for CC.

Materials and methods

Study design

In this study, 36 patients with newly diagnosed CC (clinical stage IB1–IV with visible, exophytic, endophytic, ulcerative and cauliflower-shaped tumors observed on speculum examination) admitted to the Third Affiliated Hospital of Kunming Medical University (Kunming, China) between November 2021 and March 2022 were recruited. Informed consent was obtained from each participant and the study was approved by the Institutional Review Board (NO. KYSC202161) and conducted in accordance with the ethical standards laid down in the Declaration of Helsinki. CC cases were staged according to the 2018 FIGO staging system. The following eligibility criteria were applied: (1) patient age ≥ 20 and ≤ 75 years; (2) tumors histologically confirmed as cervical squamous carcinoma, and adenocarcinoma; (3) without a second tumor; (4) had not received anti-tumor treatment before admission; (5) without exposure to any antibiotics, probiotics or steroids within four weeks prior to sample collection; (6) Karnofsky score ≥ 80 . Pathological classification of cervical tumors was performed according to the World Health Organization (WHO) Classification of Female Genital Tumors (5th edition, 2020), using a combination of hematoxylin and eosin (HE) staining and immunohistochemistry.

Treatment

Eligible patients received pelvic EBRT and brachytherapy. The EBRT dose prescribed according to the clinical target volume was 45.0–50.4 Gy delivered in 25–28 fractions of 1.8–2.0 Gy as volumetric modulated arc therapy (VMAT), or intensity-modulated radiotherapy (IMRT). Most patients (27 of 36, 75%) were treated with

concurrent weekly cisplatin/nedaplatin/carboplatin chemotherapy at a dose of 40 mg/m² for four to six cycles, whereas 25% (9 of 36) received definitive radiation therapy without concurrent chemotherapy (CCT) for reasons of personal preference or in accordance with their age and physical condition. All patients received high-dose rate intracavity brachytherapy consisting of 28.0–30.0 Gy in 4–5 fractions beginning at week five of external radiotherapy.

Tumor volume measurement and evaluation of EBRT efficacy

Two serial magnetic resonance imaging (MRI) examinations were performed at the start of EBRT (pre-EBRT), and at the time-point before starting intracavitary radiotherapy (post-EBRT). In each of the two MRI examinations, two radiation oncologists defined the tumor areas in each slice based on the T2-weighted images. Tumor volume for each of the MRIs was calculated as the sum of all tumor areas multiplied by the slice profile. For quality control, the contouring process was independently reviewed by an experienced radiologist who was blinded to the patients' treatment and group status to ensure an unbiased assessment. For each patient, pre-EBRT tumor volume (V1), and post-EBRT residual tumor volume (V2) were recorded. TVRR was defined as the percentage decrease in the tumor volume on the post-EBRT MRI scan relative to the pre-EBRT MRI scan [TVRR = (V1–V2/V1)]. According to a previous study [16], we used TVRR=66.7% as the EBRT cut-off value for CC in this study, and classified patients with TVRR≥66.7% as the SR group and those with TVRR<66.7% as the IR group.

Follow-up

The follow-up cut-off was June 24, 2023. The endpoint of this study was progression-free survival (PFS) and overall survival (OS). PFS was defined as the time interval between the initial CC diagnosis and the date of the first disease recurrence/progression or the last date of follow-up if censored. OS was defined as time interval between the initial CC diagnosis and the date of death due to CC or the last follow-up.

Sample collection and DNA extraction

Cervical tumor tissues were obtained at biopsy. Cervico-vaginal fluid samples were collected from cervical lesions using swabs. Participants were instructed in the correct technique for self-collection of stool and midstream clean-catch urine samples using sterile 50-mL centrifuge tubes (Thermo). Oral microbial samples were collected using swabs on the buccal mucosa. Participants were instructed to avoid eating/drinking for 2 h before oral sample collection. All samples were collected between

diagnosis and prior to radiotherapy, immediately frozen in liquid nitrogen, and stored at -80°C. A total of 178 specimens were collected from 36 cases (tumor tissue, stool, and oral swab) and 35 cases (vaginal swab and urine), with one vaginal swab and one urine specimen not collected due to participants being unable to provide it on schedule. According to the guideline recommended by the manufacturer, bacterial genomic DNA was extracted using the HiPure Bacterial DNA Extraction Kit (Magen, Guangzhou, China) and quantified with NanoDrop One (Thermo).

16S rRNA gene sequencing and sequence data processing

The 16S rRNA V3-V4 region was amplified by PCR using the forward 341 F (5'-CCTACGGGNGGCWGCAG-3') and the reverse primer 806R (5'-GGACTA CHVGGGTATCTAAT-3') [17]. Amplification products were recovered from 2% agarose gels, purified using the AxyPrep DNA Gel Extraction Kit (Axygen Biosciences, USA) following the manufacturer's protocols and quantitated using the ABI StepOnePlus Real-Time PCR system (Life Technologies, Foster City, USA). The purified products were pooled in equimolar amounts and subjected to paired-end sequenced (PE250) on the Illumina platform following standard protocols.

To obtain high-quality clean reads, raw reads were further filtered (version 0.18.0) by first removing reads containing more than 10% of unknown nucleotides (N) and then removing reads with less than 50% of bases having a quality (Q-value) greater than 20 using FASTP [18]. Paired-end clean reads were amalgamated into raw tags using FLSAH [19] (version 1.2.11) that overlap a minimum of 10 bp and a mismatch error rate of 2%. To obtain high-quality clean tags, noisy sequencing reads were filtered according to the following criteria: (a) raw tags were truncated at the first position where a stretch of consecutive low-quality bases (quality≤3 by default) reached a length of 3 bp; and (b) tags were filtered if they contained consecutive high-quality bases with lengths less than or equal to 75% of the tag's total length [20].

Aggregating all effective tags into operational taxonomic units (OTUs) with a similarity of ≥97% by using the UPARSE [21] (version 9.2.64) pipeline. Using the UCHIME [22] algorithm to remove all chimeric tags, resulting in the final effective tags to be analyzed further. In each cluster, those tags sequencing with the highest abundance were chosen as representations of the sequences. With the confidence threshold value of 0.8, the representative OTU sequencings were taxonomized into organisms using a naïve Bayesian model via the RDP classifier [23] (version 2.2) based on the SILVA database [24] (version 138.1). Taxonomic classification were conducted through BLAST [25] (version 2.6.0) searches of the representative OTU sequences against the NCBI 16S

ribosomal RNA Database (version 202101) to determine the specific composition of each sample at the kingdom, phylum, order, family, genus, and species levels with the best hit and strict criteria. If no BLAST hit was retained, the sequence was labeled as unclassified.

All procedures were accomplished by Gene Denovo Biotechnology (Guangzhou, China). Bioinformatic analysis was performed using Omicsmart, a platform for analyzing data online in a dynamic, real-time, and interactive way (<http://www.omicsmart.com>). The raw data of this study has been archived in the NCBI Sequence Read Archive (SRA) database and is currently available (accession number: PRJNA1086133).

Microbial diversity metrics and indicator species analysis

We characterized differences in species diversity within the specific communities of the SR and IR groups using three different alpha diversity metrics. The ACE richness index indicates the number of predicted OTUs [26]. The Pielou evenness index reflects the ratio of individual species represented in the sample population [27]. The Shannon diversity index is a comprehensive indicator to reflect the level of richness and evenness within the sample taxa [26, 27]. The ACE, Pielou, and Shannon indexes were performed using QIIME [28] (version 1.9.1). Comparisons of Alpha indexes between groups were performed using the Wilcoxon rank test in the R project Vegan package. Unweighted (phylogenetic relatedness distance) and weighted uniFrac distances (the abundance of taxa and phylogenetic relatedness distance) were applied to create the coordinates of each sample. Principle coordinate analysis (PCoA) was used to compare beta (between sample) diversity by permutational multivariate analysis of variance (PERMANOVA) using the R project Vegan package. PCoA of Unweighted and Weighted uniFrac distances were created using the R project Vegan package and plotted with the ggplot2 package. Linear discriminant analysis (LDA) effect size (LEfSe) was determined to distinguish the specific bacterial taxa that were differently enriched in the SR and IR groups. Biomarker characteristics of each group were screened by LEfSe software [29] (version 1.0). An LDA score threshold was set at 3.0, and $p < 0.05$ was deemed to be statistically significant.

Immunohistochemistry and HE staining

Cervical tumor tissues were fixed by 4% paraformaldehyde, sectioned into 4- μ m-thick paraffin-embedded sections, then mounted on Adhesive Slides (MXB Biotechnologies). Sections were deparaffinized in xylene and rehydrated through graded ethanol. Addition of antigen retrieval was performed in citrate buffer (citrate pH 6.0) with microwave heating. Endogenous peroxidase was inactivated, and sections were blocked with 5% goat serum, then incubated with primary antibodies for

detection of CD8 (CD8 T cells) (ZSGB-BIO ZA-0508, China) (ready-to-use reagents) and Granzyme B (GzmB) (ZSGB-BIO ZA-0599, China) (ready-to-use reagents) overnight at 4 °C. And next day the sections were incubated with the secondary antibody (ZSGB-BIO Horseradish-peroxidase-conjugated Goat anti-rabbit/mouse IgG Antibody PV-8000, China) (ready-to-use reagents) at room temperature, followed by detection using DAB substrate and hematoxylin counterstaining. Slides were mounted on the microscope (DM400B, LEICA) and visualized by INFINITY CAPTURE application (version 5.0.4). Positively stained cells were quantified in five stochastic areas (1 mm² each) of the tumor, and the density of cells expressing CD8 and GzmB was measured [10]. The mean total number of cells positive for each marker in each of the five regions was expressed as a density per mm². To confirm the specificity of the immunostaining, sections without the primary antibody were used as a negative control. Normal spleen tissue was used as a positive control for the marker. The sections were additionally stained using haematoxylin and eosin (HE). For HE staining, sections were deparaffinized in xylene, rehydrated through a series of anhydrous ethanol and graded ethanol solutions (95%, 85%, and 75%), stained with hematoxylin, differentiated in 1% hydrochloric acid, counterstained with eosin, dehydrated, cleared in xylene, and then mounted. Positive controls, negative controls, and HE sections are shown in Supplement Fig. 1.

Statistical analysis

Statistical analysis was performed using the program SPSS 26.0 software (IBM, Chicago, IL, USA), GraphPad Prism 9 software (San Diego, CA), and R software (version 4.2.1). Partial results were derived from Omicsmart. We employed descriptive statistics to recapitulate the clinical characteristics and demographic of the patients. Categorical data were expressed as numbers (percentages). Continuous variables were expressed as the median and interquartile range (IQR). Comparisons of categorical variables were performed using Fisher's exact test. Comparisons of continuous variables were done using Wilcoxon rank-sum test. In this study, we employ the least absolute shrinkage and selection operator (LASSO) logistic regression method to assess the impact of potential confounding factors on the efficacy of EBRT. All clinicopathological factors were analysed by LASSO regression method. The LASSO regression analysis was performed using the R package "glmnet". The standard lambda (λ) value was established by identifying the value that yielded the minimum error through 10-fold cross-validation. The logistic regression algorithm was used to test the significant of the most relevant confounding factor. Two-tailed Wilcoxon rank-sum tests were used to analyze the ACE, Shannon, and Pielou indexes, and

to compare differences in the expression of CD8 and GzmB between the SR and IR groups. PERMANOVA was used to compare beta diversity between samples. The Spearman test was used for correlation analysis. The correlation heatmaps were plotted using the “corrplot” R package. Receiver operator characteristic (ROC) and area under curve (AUC) analyses were used to evaluate the prediction effectiveness of specific microbial taxa as biomarkers. X-tile software (Yale University School of Medicine, USA) (version 3.6.1) was used to identify the optimal cut-off values based on the highest χ^2 value [30]. Survival curves were plotted using the Kaplan-Meier method and compared using the log-rank test. $P < 0.05$ was considered to indicate statistical significance.

Results

Demographics

The clinicopathologic characteristics of 36 CC patients in this study are shown in Table 1. There were 26 patients in the SR group and 10 patients in the IR group, with no significant differences in the distributions of age ($p = 1.000$), 2018 FIGO staging system ($p = 1.000$), histological type ($p = 0.370$), histological differentiation ($p = 0.608$), maximal tumor size ($p = 0.155$), lymph nodes metastases ($p = 0.463$), HPV status ($p = 0.597$), body mass index ($p = 0.549$), menstrual status ($p = 0.438$), hypertension history ($p = 1.000$), diabetes history ($p = 0.181$), marital status ($p = 0.545$), socioeconomic status ($p = 0.708$), and EBRT treatment modality ($p = 0.686$) between the two groups. All patients had no history of smoking or alcohol consumption.

To assess the potential impact of clinicopathologic characteristics on EBRT, we used the LASSO regression method to select the most relevant factors from the 14 variables mentioned above and identified 1 variable that was most relevant with EBRT efficacy, which was diabetes history (Supplement Fig. 2A-B). Univariate logistic analysis was then performed to evaluate the significance of this variable and found that diabetes history ($p = 0.156$) was not associated with EBRT efficacy (Supplement Table 1). The result indicated that the classification into SR and IR groups based on EBRT efficacy was not influenced by clinicopathologic characteristics.

Identification of specific microbiome taxa associated with EBRT efficacy

To identify specific microbiome taxa associated with EBRT efficacy, we first compared the alpha diversity of the multi-site microbiota of the SR group with that of the IR group. Compared to the IR group, the alpha diversity of the tumor microbiome was significantly lower in the SR group, as indicated by Shannon and Pielou indexes ($p = 0.011$ and $p = 0.019$, respectively, Fig. 1A, Supplement Table 2). The ACE index revealed the same pattern,

with the ACE index being lower in the SR group of tumor microbiomes as compared to the IR group, although there was no statistical difference ($p = 0.286$, Fig. 1A, Supplement Table 2). And there were no significant differences in alpha diversity of the vaginal, gut, urethral, and oral microbiomes between the SR and IR groups (Supplement Fig. 3A-D, Supplement Table 2).

Analysis of the beta diversity, which accounts for differences in taxon abundance and phylogenetic relatedness, revealed significant differences in the gut microbiome abundance in the SR and IR groups at the baseline level ($p = 0.039$, Supplement Fig. 3F, Supplement Table 3). Phylogenetic closeness was detected among the microbial communities of the tumor, vaginal, gut, urethral, and oral samples of the SR and IR groups (Fig. 1B, Supplement Fig. 3E-H, Supplement Table 3).

Aiming to accurately identify microorganisms that could predict EBRT efficacy, we assessed the potential influences of major clinicopathological factors on microbial diversity, pathological type, maximum tumor size, the status of lymph node metastasis, and EBRT treatment modality with or without CCT. We found that, in addition to the intra-tumoral microbiome, the microbiome diversity of the vaginal, gut, urethral, and oral samples was affected by clinico-pathological features (Supplement Figs. 4 and 5). These results indicated that the composition of intra-tumoral microorganisms was relatively stable and poorly related to clinico-pathological features, so that screening of specific intra-tumoral microbiome taxa associated with EBRT efficacy would be more reliable. We then conducted high dimensional class comparisons using LEfSe to detect marked differences in the predominance of bacterial communities between these two intra-tumoral groups (Fig. 1C-D). The SR group tumors were characterized by predominance of *Bifidobacteriaceae*, *Beijerinckiaceae*, and *Orbaceae* at the family level. In contrast, the tumors of the IR group were dominated at the family level by other 13 bacteria, including *Sphingomonadaceae*, *Caulobacteraceae*, *Pseudonocardiaceae*, and *Rhizobiaceae*.

Specific bacterial taxa and EBRT efficacy

The intra-tumoral microbiota plays a lynchpin role in shaping the host's immune system. A recent investigation showed that the specific intra-tumoral microbiota composition can improve the anti-tumor immune response via facilitating CD8⁺ T cells recruitment and activation [10]. Therefore, we hypothesized that intra-tumoral microbiome may be associated with the tumor immune microenvironment, which may influence the efficacy of EBRT in patients with CC. To confirm our speculation, we used immunohistochemistry to determine the intra-tumoral immune infiltrates in this cohort. We found higher densities of CD8⁺ T and GzmB⁺ cells in

Table 1 Clinical and pathological characteristics of the study population

Characteristics	Whole sample (n = 36)	IR group (n = 10)	SR group (n = 26)	p
Age at diagnosis (years, IQR) ^a	55.50 (49.00-66.75)	51.50 (50.00-68.25)	56.50 (45.00-66.75)	0.764 ^c
Age at diagnosis, n (%) ^b				1.000 ^d
≤ 50years	14 (38.9)	4 (28.6)	10 (71.4)	
> 50years	22 (61.1)	6 (27.3)	16 (72.7)	
FIGO stage (2018), n (%) ^b				1.000 ^d
IA-IIA	2 (5.6)	0 (0.0)	2 (100.0)	
IIB-IVB	34 (94.4)	10 (29.4)	24 (70.6)	
Histological type, n (%) ^b				0.370 ^d
Squamous cell carcinoma	29 (80.6)	7 (24.1)	22 (75.9)	
Adenocarcinoma	7 (19.4)	3 (42.9)	4 (57.1)	
Histological differentiation, n (%) ^b				0.608 ^d
G1 well-differentiated	3 (8.3)	1 (33.3)	2 (66.7)	
G2 moderately-differentiated	15 (41.7)	6 (40.0)	9 (60.0)	
G3 poorly- differentiated	3 (8.3)	0 (0.0)	3 (100.0)	
Unknown	15 (41.7)	3 (20.0)	12 (80.0)	
Maximal tumor size (cm, IQR) ^a	5.35 (4.03–6.98)	5.55 (4.63–7.48)	5.30 (3.98–6.90)	0.243 ^c
Maximal tumor size (cm), n (%) ^b				0.155 ^d
≤ 4	7 (19.4)	0 (0.0)	7 (100.0)	
> 4	29 (80.6)	10 (34.5)	19 (65.5)	
Lymph nodes metastases, n (%) ^b				0.463 ^d
Yes	17 (47.2)	6 (35.3)	11 (64.7)	
No	19 (52.8)	4 (21.1)	15 (78.9)	
HPV status, n (%) ^b				0.597 ^d
Positive	18 (50.0)	4 (22.2)	14 (77.8)	
Negative	2 (5.6)	1 (50.0)	1 (50.0)	
Unknown	16 (44.4)	5 (31.3)	11 (68.7)	
BMI ^b				0.549 ^d
≤ 18.5	2 (5.6)	0 (0.0)	2 (100.0)	
18.5 < BMI ≤ 25	20 (55.6)	5 (25.0)	15 (75.0)	
25 < BMI ≤ 30	12 (33.3)	5 (41.7)	7 (58.3)	
> 30	2 (5.6)	0 (0.0)	2 (100.0)	
Menstrual status ^b				0.438 ^d
Pre- menopausal status	12 (33.3)	2 (16.7)	10 (83.3)	
Post-menopausal status	24 (66.7)	8 (33.3)	16 (66.7)	
Hypertension history ^b				1.000 ^d
No	25 (69.4)	7 (28.0)	18 (72.0)	
Yes	11 (30.6)	3 (27.3)	8 (72.7)	
Diabetes history ^b				0.181 ^d
No	33 (91.7)	8 (24.2)	25 (75.8)	
Yes	3 (8.3)	2 (66.7)	1 (33.3)	
Marital status ^b				0.545 ^d
Married	33 (91.7)	10 (30.3)	23 (69.7)	
Divorced	3 (8.3)	0 (0.0)	3 (100.0)	
Socioeconomic status ^b				0.708 ^d
Lower	9 (25.0)	2 (22.2)	7 (77.8)	
Middle	17 (47.2)	6 (35.3)	11 (64.7)	
Upper	10 (27.8)	2 (20.0)	8 (80.0)	
EBRT treatment modality ^b				0.686 ^d

Table 1 (continued)

Characteristics	Whole sample (n = 36)	IR group (n = 10)	SR group (n = 26)	p
With CCT	27(75.0)	7(25.9)	20(74.1)	
Without CCT	9(25.0)	3(33.3)	6(66.7)	

Abbreviations: IQR, interquartile range; FIGO, International Federation of Gynecology and Obstetrics; SR, superior response; IR, inferior response; HPV, human papilloma virus infection; BMI, body mass index; EBRT, external beam radiation therapy; CCT, concurrent chemotherapy.

Data are presented as numbers median (interquartile range)^a or (percentages)^b.

^cp-value was calculated using Wilcoxon rank-sum test.

^dp-value was calculated using Fisher's exact test.

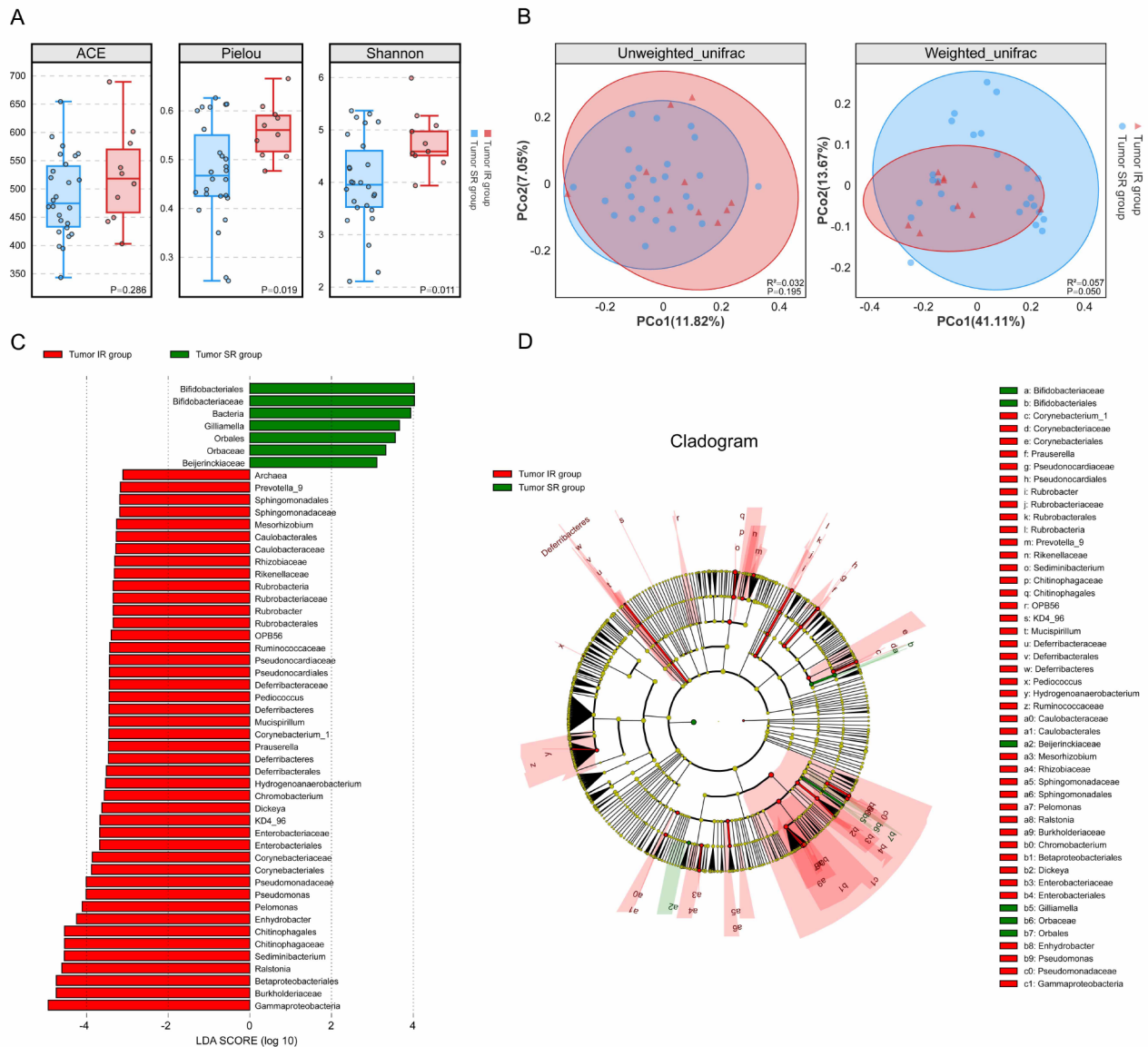


Fig. 1 Intra-tumoral microbiome diversity and communities differ significantly between the SR and IR groups of cervical cancer patients. **(A-B)** Alpha diversity boxplot (ACE, Pielou and Shannon) **(A)** and principal coordinate analysis (PCoA) of beta diversity using Unweighted and Weighted Unifrac **(B)** for cervical cancer intra-tumoral microbiome. **(C-D)** LefSe analysis identification of intra-tumoral microbiome biomarkers between the IR and SR groups. **(C)** Linear discriminant analysis (LDA) scores computed for differentially abundant taxa in the intra-tumoral microbiomes of the IR (red) and SR (green) groups. Feature selection criteria: log LDA score > 3.0. **(D)** Taxonomic cladogram showing taxonomic association of microbiomes between the IR and SR groups. Each node represents a specific taxonomic type. Green nodes denote the taxonomic types that are more abundant in the SR group, while the red nodes represent the taxonomic types that are more abundant in the IR group. Yellow nodes denote the taxonomic features with no significant differences between the IR and SR groups. SR, superior response; IR, inferior response

the SR group comparison to the IR group ($p=0.0002$ and $p=0.0036$, respectively) (Fig. 2A).

Spearman rank-order correlation analysis revealed a significantly positive correlation between the tumor densities of CD8⁺ T and GzmB⁺ cells and the TVRR of patients ($p=0.0004$ and $p=0.0206$, respectively) (Fig. 2B). We then analyzed the correlation of the CD8⁺ T and GzmB⁺ cells tumor tissue densities with the specific enriched family in the SR group patients (*Bifidobacteriaceae*, *Beijerinckiaceae*, and *Orbaceae*). We found a positive Spearman correlation between the CD8⁺ T and GzmB⁺ cell tumor tissue densities and *Bifidobacteriaceae* ($p=0.0097$ and $p=0.0119$, respectively), while no significant correlation were detected for the other two families ($p=0.7873$ and $p=0.2719$; $p=0.0579$ and $p=0.2143$, respectively) (Fig. 2C-E). Meanwhile, we found a strong negative correlation between the Pielou and Shannon indexes and TVRR ($p=0.0017$ and $p=0.0006$, respectively), and a negative correlation between the ACE index and TVRR ($p=0.1220$, Fig. 2F), although the correlation did not reach the level of statistical significance. Finally, we analyzed the correlations of the CD8⁺ T and GzmB⁺ cell tumor tissue densities with the three alpha diversity indexes. We found a significant negative correlation with ACE index ($p=0.0090$ and $p=0.0380$, respectively), and the same negative correlation with Pielou and Shannon indexes, although the correlations were not statistically significant ($p=0.1050$ and $p=0.1415$; $p=0.0791$ and $p=0.1367$, respectively) (Fig. 2G). The heatmap of the correlation of these intra-tumoral microbial parameters with TVRR, CD8⁺ T, and GzmB⁺ cell were shown in Fig. 2H-I.

The intra-tumoral microbiome might participate various cellular processes like gene expression regulation, metabolic manipulation, protein secretion or human leukocyte antigen (HLA) mediated antigen presentation [31]. During these processes, tumor cells might remodel the microenvironment and release signals to attract peripheral immune cells. Our findings indicate that a higher abundance of *Bifidobacteriaceae* and lower alpha diversity within tumors may facilitate the recruitment and activation of CD8⁺ T cells in the tumor microenvironment (TME), leading to enhanced anti-tumor immune responses. This favorable immunological landscape, in conjunction with EBRT, may synergistically contribute to tumor cell destruction, ultimately yielding better treatment outcomes for patients with CC.

Specific bacterial taxa predict EBRT efficacy

We used these three families with higher abundances in the SR group to perform ROC analysis of the performance of these families in predicting EBRT efficacy. (Fig. 3A). We found that the AUCs were 0.719 (95% confidence interval [CI], 0.537–0.901), 0.750 (95% CI,

0.581–0.919) and 0.696 (95% CI, 0.572–0.821) for *Bifidobacteriaceae*, *Beijerinckiaceae*, and *Orbaceae*, respectively. However, combining these three taxa resulted in an AUC of 0.831 (95%CI, 0.667–0.995), suggesting that the relative abundance of *Bifidobacteriaceae*, *Beijerinckiaceae*, and *Orbaceae* as specific taxa within the tumor may have potential as a biomarker for predicting the efficacy of EBRT in CC.

To explore how the intra-tumoral microbiome affects patient treatment, we then used X-tile software to determine the optimal cut-off values of the Shannon index and relative abundance of *Bifidobacteriaceae*, stratifying patients into high versus low categories based on these optimal cut-off values. Kaplan-Meier survival curves plotted according to the Shannon index and relative abundance of *Bifidobacteriaceae* (Fig. 3B-C) showed that better PFS and OS outcomes were predicted for CC patients with a lower Shannon index (hazard ratio [HR]=4.684, 95% CI, 0.903–24.302; HR=14.067, 95%CI, 0.315–627.299) and higher abundance of *Bifidobacteriaceae* (HR=3.001, 95% CI, 0.803–11.217; HR=6.115, 95% CI, 0.626–59.690). These results indicate that the intra-tumoral microbiome alpha diversity and the abundance of *Bifidobacteriaceae* may serve as promising predictors of treatment outcome in CC patients. However, further research is required to elucidate the molecular mechanisms by which the intra-tumoral microbiome influences treatment efficacy, thereby informing the development of novel personalized treatment strategies.

Discussion

In this prospective analysis, we used 16S rRNA sequencing to analyze the microbiome within cervical tumor tissues and found that intra-tumoral specific microbiome taxa (*Bifidobacteriaceae*, *Beijerinckiaceae*, and *Orbaceae*) and lower alpha diversity were associated with better EBRT outcomes. As far as we know, this is the first molecular ecological research exploring the relationship between the intra-tumoral microbiome and EBRT outcomes using a deep sequencing approach.

Radiotherapy resistance is the main cause of poor prognosis in CC patients. The therapeutic effect of radiotherapy is often limited by inherent physiological barriers of TME, including hypoxia [32] and an immunosuppressive TME [33]. Thus, new strategies to synergize radiotherapy that can reshape the TME to overcome radiation-resistance are urgently required.

In 2022, the human polymorphic microbiome, which includes the intra-tumoral microbiome and the commensal microbiome of other anatomical sites, was identified as one of the latest “hallmarks of cancer” [34], highlighting the crucial role of the intra-tumoral microbiome in modulating cancer susceptibility and tumor progression. Sun et al. reported that the intra-tumoral microbiome

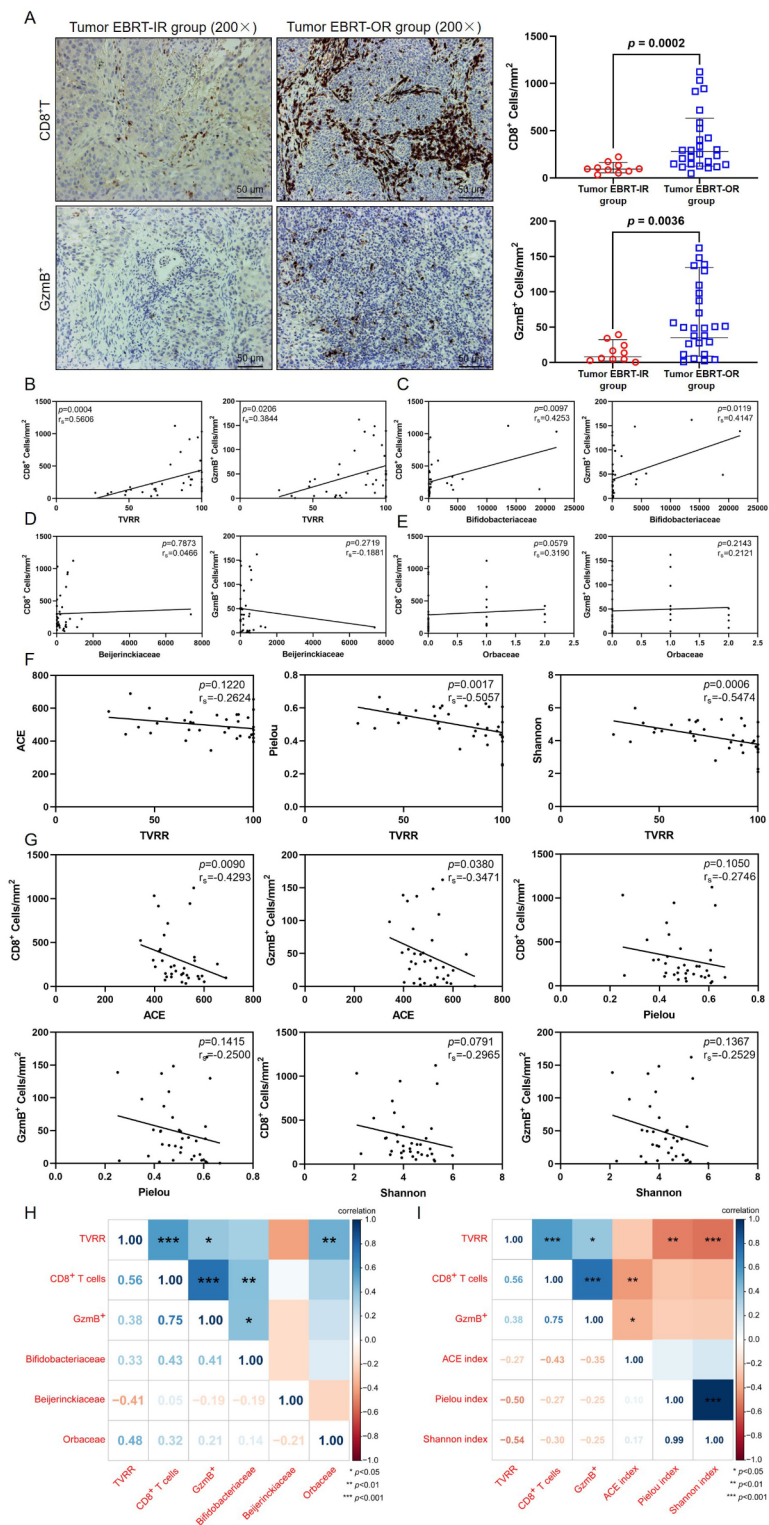


Fig. 2 Higher intra-tumoral relative abundance of *Bifidobacteriaceae* and lower microbiome alpha diversity in patients with cervical cancer are significantly associate with strong immune infiltration. **(A)** Immunohistochemical (IHC) staining of CD8 and GzmB from tumors of IR and SR group patients (representative image, 200× magnification) (left) and quantification of IHC signal of CD8⁺, and GzmB⁺ from tumors of IR and SR group patients (right). Scale bar, 50 μm. **(B)** Spearman correlation between CD8⁺ and GzmB⁺ tissue densities and TVRR. **(C-E)** Spearman correlation between CD8⁺ and GzmB⁺ tissue densities and **(C)** *Bifidobacteriaceae*, **(D)** *Beijerinckiaceae*, **(E)** and *Orbaceae* in cervical cancer patients. **(F)** Spearman correlation between ACE, Pielou and Shannon indexes and TVRR in cervical cancer patients. **(G)** Spearman correlation between CD8⁺ and GzmB⁺ tissue densities and ACE, Pielou and Shannon indexes in cervical cancer patients. **(H)** The correlations of TVRR, CD8⁺, GzmB⁺, *Bifidobacteriaceae*, *Beijerinckiaceae*, and *Orbaceae*. **(I)** The correlations of TVRR, CD8⁺, GzmB⁺, ACE index, Pielou index and Shannon indexes. SR, superior response; IR, inferior response; GzmB, granzyme B; TVRR, tumor volume reduction rate

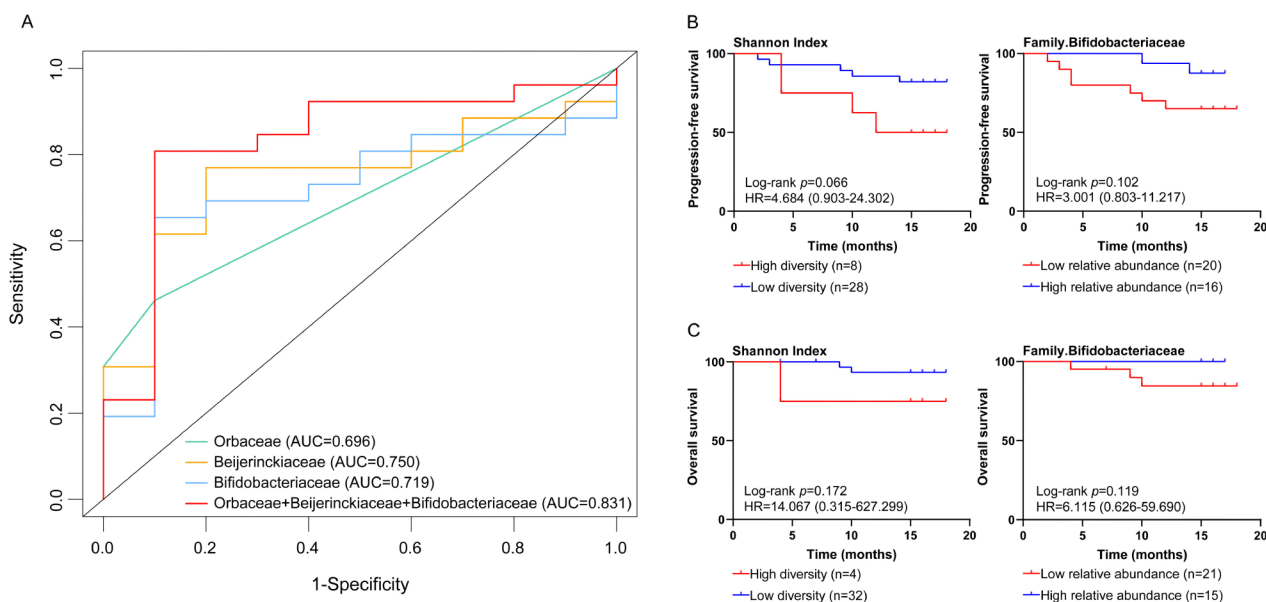


Fig. 3 The intra-tumoral microbiome has the potential to predict the response to external beam radiation therapy in cervical cancer. **(A)** Receiver operator characteristic analysis of intra-tumoral specific microbiome taxa relative abundance as a predictor of superior response status. **(B-C)** Kaplan-Meier (KM) curves of progression-free survival (PFS) and overall survival (OS) determined by log-rank tests of patients with low (blue) or high (red) Shannon indexes (left curve) or with high relative abundance (blue) or low relative abundance (red) of *Bifidobacteriaceae* (right curve). **(B)** KM curves of PFS. **(C)** KM curves of OS

can predict the postoperative prognosis of patients with hepatocellular carcinoma [35]. Zhang et al. demonstrated that the intra-tumoral microbiome impacts the efficacy of first-line treatments and survival in patients with non-small cell lung cancer that are free of lung infections [36]. Furthermore, Nejman et al. showed that diversity and composition of the intra-tumoral microbiome in pancreatic ductal adenocarcinoma can influence immune infiltration and ultimately, affect the long-term prognosis of patients [7, 8]. These data suggest that microbiological factors, irrelevant to the tumoral genomic composition, may determine patient prognosis. Similarly, in this study, we identified the presence of specific intra-tumoral microbiome taxa and lower alpha diversity in CC patients achieving better EBRT treatment and superior PFS and OS outcomes.

Bifidobacteriaceae is a Gram-positive (G+) obligate anaerobic probiotic that colonizes the intestinal tract, oral cavity, and vagina in humans. *Bifidobacteriaceae* has been shown to induce therapeutic and anti-cancer effects against tumor lesions in tumor-bearing animal models. Abdolalipour et al. [37] found that by intravenously or orally administering *Bifidobacterium bifidum* was effective in inducing anti-tumor immune responses and inhibiting tumor growth in C57BL/6 mice transplanted with human papillomavirus-associated tumor TC-1 cells. In addition, intravenous administration of the probiotic *Bifidobacterium bifidum* resulted in the activation of tumor-specific IFN- γ and IL-12, lymphocyte proliferation, and

CD8⁺ cytolytic responses that control and eradicate tumor growth in tumor-bearing mice. Sivan et al. [38] demonstrated significantly improved tumor control in mice treated with *Bifidobacterium* in comparison with their untreated counterparts. In addition, the tumor control in this model was accompanied by increasing cumulation of antigen-specific CD8⁺ T cells present in the tumor and peripheral tumor-specific T cells that were robustly induced. Their findings suggested that *Bifidobacterium*-derived signals modulate the activation of dendritic cells in the steady state, which in turn leads to enhanced CD8⁺ T cell priming and cumulation in TME to mediate tumor control. However, researches on the characteristics of *Bifidobacteriaceae* in the cervical cancer microbiome were in its infancy. Cha et al. [39] investigated the antiviral effects of *Bifidobacterium adolescentis* SPM1005-A in the SiHa cervical cancer cell line expressing HPV type 16, and identified that the *Bifidobacterium* strain had antiviral activity via suppression of E6 and E7 oncogene expression. Chao et al. [40] explored the potential vaginal microbiome biomarkers that may lead to high-grade squamous intraepithelial lesion (HSIL), and identified that a paucity of *Bifidobacterium*, *Faecalibacterium*, *unidentified Prevotellaceae*, *Bacteroides*, and *Dialister* were related with HSIL. The relative abundance of *Bifidobacterium* being under 0.0116183% maybe a potentially good predictor of HSIL in HPV16 and/or 18 infected individuals. In another research, cervical lesions were reported to be associated with four bacterial

genera characterized by being in low abundance (*Bifidobacterium*, *Aerococcus*, *Moryella*, and *Schlegella*) and one that maintained high abundance (*Gardnerella*) [41]. Our results showed a significant positive correlation between the intra-tumoral enrichment of *Bifidobacteriaceae* and infiltrate densities of CD8⁺T and GzmB⁺, which suggested that the higher abundance of *Bifidobacteriaceae* within CC tumor tissues may enhance anti-tumor immunity by recruiting and activating CD8⁺T cells, facilitating improved treatment outcomes in patients who receive radiotherapy. However, investigations on the role of *Bifidobacteriaceae* in the intra-tumoral microbiota were still very insufficient. Notably, we found that specific intra-tumoral microbiome taxa consisting of *Bifidobacteriaceae*, *Beijerinckiaceae*, and *Orbaceae* were highly predictive of the therapeutic efficacy of EBRT. Very little is currently known about potential fluctuations in *Beijerinckiaceae* and *Orbaceae*, which may yield superior therapeutic outcomes through generating prebiotics or otherwise, and requires more insightful investigation in the future to elucidate the mechanisms involved. Additionally, there remains a large number of microbes in TME that do not exhibit significant differences in abundance. Determining whether these microbes act as promoters, inhibitors, or neutral entities within TME requires further investigation. In-depth exploration of the interactions between these microbes and host tumor cells will enable more accurate characterization of potential microbial markers composed of specific microbial taxa, providing new opportunities for individualized precision therapy.

Alpha diversity is an essential metric for evaluating diversity differences within samples and has been widely used in microbial research [42]. Wang et al. [43] examined the diversity of vaginal microbiota in women with locally advanced cervical cancer and evaluated the differences between responders and nonresponders. They found that there was significantly higher alpha diversity in vaginal samples of nonresponders as compared with responders ($p < 0.01$) and alpha diversity may have the potential ability to identify early platinum-resistant patients. Our finding suggests that the alpha diversity of the intra-tumoral microbiome of CC was negatively correlated with infiltrate densities of CD8⁺ T cells and GzmB⁺, and patients with lower alpha diversity achieved a better prognosis. This may be explained by the closeness of the cervical tumor to the vaginal environment, in which the development of pre-cancerous lesions and progression to CC is accompanied by a dramatic reduction in *Lactobacillus* among the vaginal microorganisms and markedly increased levels of microbial diversity [44–46]. Although the lower microbial diversity may have immunomodulatory effects, its role in anti-neoplastic responses is not completely clear. We speculate that the

lower alpha diversity implies a relatively more simplified composition of the intra-tumor microbiome, with comparatively fewer harmful microorganism components, which may be more conducive to CD8⁺ T cell recruitment and activation.

Through rigorous inclusion and exclusion criteria, our study found no association between intra-tumoral microbiome characteristics and clinicopathological factors in patients with cervical cancer who had not received antibiotic treatment within four weeks. Nonetheless, in clinical practice, antibiotics can significantly impact the human microbiome. A study has shown that antibiotic therapy, by reducing the load of intra-tumoral bacteria in pancreatic cancer, can decrease the recruitment of suppressive cells while increasing the recruitment of innate effector cells and enhancing cytolytic T cell activity [47]. It is indisputably uplifting to attain such results. However, systemic antibiotic administration in practical applications may raise concerns about antibiotic overuse. Therefore, developing novel antibiotic treatment strategies targeting intra-tumoral bacteria could have a significantly positive impact on cancer therapy. By characterizing the composition of the tumor microbiome prior to treatment and selectively administering antibiotics intra-tumorally to eliminate bacteria that inhibit antitumor effects, while introducing bacteria that enhance antitumor efficacy into the TME, the host's response to treatment can be optimized. In addition to antibiotic approaches, the development of methods such as probiotics, bacteriophages, and microbiome editing to remodel the intra-tumoral microbiota has emerged as promising potential therapeutic tactics. Probiotics have been suggested as a means to positively influence the diversity of a specific microbiome. Administering *Bifidobacterium* species orally to melanoma-bearing mice demonstrated equivalent efficacy to PD-L1 inhibitor treatment, and enhanced the inhibitor's effectiveness when used adjunctively by augmenting the quantity and accumulation of primed T cells in tumor [38]. Bacteriophages, as the viruses that infect bacteria, have the ability to selectively destroy them. In preclinical studies, bacteriophages have been shown to exhibit similar efficacy against specific bacterial taxa as antibiotics, with less damage to non-target commensal bacteria [48]. Some scientists have identified several *Fusobacterium*-targeted bacteriophages capable of penetrating tumors and targeting the resident bacteria following intravenous administration in mice [49]. Another innovative strategy for targeting tumor microbiota is microbiome editing. This strategy utilizes bioengineering techniques to create microorganisms or its specific antibodies that can be directly targeting and destroying tumor cells. The treatment of non-muscle-invasive bladder cancer with *Bacille Calmette-Guérin* (BCG) and the use of the oncolytic virus talimogene laherparepvec (T-VEC) for advanced

melanoma illustrate successful regulation of the tumor microbe microenvironment through microbiome editing techniques [50–53]. Wang et al. found that *Bifidobacterium* and its specific monoclonal antibody can warm cold tumors and improve the abscopal effect of radiotherapy [54]. However, the development and application of these novel therapeutic strategies are still immature and relying on further research. Our study provides a foundation for investigating the integration of microbial modulation strategies with radiotherapy by characterizing the specific intra-tumoral microbial features associated with the efficacy of EBRT in cervical cancer. This work also offers new avenues for research aimed at improving the efficacy of EBRT in cervical cancer.

A few limitations are noted in this study. First, our research is a single-center and small sample study with a relatively short follow-up, which limits the ability to form robust conclusions with regard to the potential association of the intra-tumoral microbiome with survival. Second, owing to the inherent limitations of next-generation sequencing technology, some low-abundance microorganisms are categorized as “unclassified”, and the impact of these unidentified microorganisms, considered to be “the human microbiome’s dark matter”, on cancer progression and treatment prognosis is still unknown [55]. However, their presence may have a “butterfly effect” on the occurrence and development of tumors. There is a need for further research and more advanced methods to explore the potential role of these low-abundance microbiomes in the future. Finally, the findings of this study remain to be validated by in vitro cellular experiments and in vivo animal experiments. Multicenter, randomized, and placebo-controlled trials are also warranted to determine the exact mechanisms by which specific microbiota activate antitumor immunity.

Conclusions

Conclusively, we found that the intra-tumoral microbiome unique to the SR group and lower alpha diversity were associated with a favorable tumor microenvironment, with characteristics of increased CD8⁺ T cell infiltration in the tumoral milieu, which may be a potential predictor for EBRT efficacy in CC patients. Results of this study broaden our understanding of the possible function of the intra-tumoral microbiome in radiation efficacy, as well as provide valuable insights into the pathophysiology and potential therapeutics for CC patients.

Abbreviations

EBRT	External beam radiation therapy
CC	Cervical cancer
SR	Superior response
IR	Inferior response
FIGO	Federation of Gynecology and Obstetrics
TVRR	Tumor volume reduction rate
VMAT	Volumetric modulated arc therapy

IMRT	Intensity-modulated radiotherapy
CCT	Concurrent chemotherapy
OS	Overall survival
PFS	Progression-free survival
MRI	Magnetic resonance imaging
OUTs	Operational taxonomic units
SRA	Sequence Read Archive
LASSO	Least absolute shrinkage and selection operator
WHO	World Health Organization
HE	Hematoxylin and eosin
LEfSe	Linear discriminant analysis effect size
LDA	Linear discriminant analysis
PCoA	Principle coordinate analysis
PERMANOVA	Permutational multivariate analysis of variance
IQR	Interquartile range
ROC	Receiver operator characteristic
AUC	Area under curve
TME	Tumor microenvironment
PDAC	Pancreatic ductal adenocarcinoma
HSIL	High-grade squamous intraepithelial lesion
HLA	Leukocyte antigen
T-VEC	Talimogene laherparepvec

Supplementary Information

The online version contains supplementary material available at <https://doi.org/10.1186/s12967-024-05774-8>.

Supplementary Material 1: Supplement Fig. 1. Representative images of positive controls, negative control and haematoxylin and eosin (HE) section. (A) Immunohistochemical (IHC) staining of CD8 and GzmB in positive control (normal spleen tissue, 100x magnification). (B) HE section, negative control (without the primary antibody), and representative images of positive expression of CD8 and GzmB markers in tumor tissue (100x magnification). Scale bar, 50 μm.

Supplementary Material 2: Supplement Fig. 2. Potential confounding factors among clinicopathological characteristics that may influence the efficacy of external beam radiation therapy were screened using LASSO regression analysis. Selection of tuning parameter (λ) in the LASSO model via 10-fold cross-validation in our cohort. (A) One potential variable (namely, Diabetes history) with non-zero coefficients were chosen in the LASSO regression analysis based on the optimal λ value. (B) The optimal λ value of 0.117 was chosen based on minimum criteria.

Supplementary Material 3: Supplement Fig. 3. Evaluation of the microbiome diversity of other body sites. (A–D) Alpha diversity boxplots (ACE, Pielou, and Shannon) of (A) vaginal, (B) gut, (C) urethral, and (D) oral microbiome samples from patients in the SR and IR groups. (E–H) Principal coordinate analysis of (E) vaginal, (F) gut, (G) urethral, and (H) oral microbiome samples by using Unweighted and Weighted uniFrac of beta diversity.

Supplementary Material 4: Supplement Fig. 4. Analysis of alpha diversity based on influencing factors. (A–E) Alpha diversity boxplots (ACE, Pielou, and Shannon) of (A) tumor, (B) vaginal, (C) gut, (D) urethral, and (E) oral microbiome samples from cervical cancer patients. Analysis of following factors: age (left1), histological type (left2), maximal tumor size (left3), lymph nodes metastases (right2), and EBRT treatment modality with or without CCT (right1). EBRT, external beam radiation therapy; CCT, concurrent chemotherapy.

Supplementary Material 5: Supplement Fig. 5. Analysis of beta diversity based on influencing factors. (A–E) Principal coordinate analysis of beta diversity in (A) tumor, (B) vaginal, (C) gut, (D) urethral, and (E) oral microbiome samples from cervical cancer patients using Unweighted and Weighted uniFrac analysis of following factors: age (left1), histological type (left2), maximal tumor size (left3), lymph nodes metastases (right2), and EBRT treatment modality with or without CCT (right1). EBRT, external beam radiation therapy; CCT, concurrent chemotherapy

Supplementary Material 6

Acknowledgements

The authors would like to appreciate to subjects who participated in this study.

Author contributions

Lan Zhang: Conceptualization, Supervision, and Project administration. Zheng Li: Methodology, Writing- Review and Editing. Zhongyan Dou: Investigation, Formal analysis, Writing- Original Draft. Conghui Ai: Data curation, Writing- Original draft preparation. Jinping Zhang: Data curation, Writing- Original draft preparation. Kangming Li and Meiping Jiang: Resources. Xingrao Wu and Chunfang Zhao: Software. All authors read and gave final approval of the version to be published.

Funding

This investigation was supported by the National Natural Science Foundation of China (81802614, 82160562), the Innovative Research Team of Yunnan Province (202305AS350020).

Data availability

The raw data from this study has been uploaded and archived in the NCBI Sequence Read Archive (SRA) database and can be viewed now (accession number: PRJNA1086133). The datasets involving clinicopathologic information on patients in this investigation can be obtained from the corresponding authors for reasonable reasons.

Declarations

Ethics approval and consent to participate

This investigation was strictly adhered to the ethical guidelines of the Declaration of Helsinki and was approved by the Research Ethics Committee of the Third Affiliated Hospital of Kunming Medical University (NO. KYSC202161). All procedures involving human participants in this investigation conformed to the ethical standards in the 1964 Declaration of Helsinki and its subsequent amendments.

Consent for publication

Not applicable.

Competing interests

All the authors of this study declare that no conflict of interest, financial or otherwise, exists in relation to the subject matter of the submitted article.

Author details

¹Department of Radiation Oncology, The Third Affiliated Hospital of Kunming Medical University (Yunnan Cancer Hospital, Yunnan Cancer Center), 519 Kunzhou Road, Kunming 650118, China

²Department of Radiology, The Third Affiliated Hospital of Kunming Medical University (Yunnan Cancer Hospital, Yunnan Cancer Center), 519 Kunzhou Road, Kunming 650118, China

³Department of Medical Administration, The Third Affiliated Hospital of Kunming Medical University (Yunnan Cancer Hospital, Yunnan Cancer Center), 519 Kunzhou Road, Kunming 650118, China

⁴Department of Gynecologic Oncology, The Third Affiliated Hospital of Kunming Medical University (Yunnan Cancer Hospital, Yunnan Cancer Center), 519 Kunzhou Road, Kunming 650118, China

Received: 3 June 2024 / Accepted: 18 October 2024

Published online: 28 October 2024

References

1. Sung H, Ferlay J, Siegel RL, Laversanne M, Soerjomataram I, Jemal A, Bray F. Global Cancer statistics 2020: GLOBOCAN estimates of incidence and Mortality Worldwide for 36 cancers in 185 countries. *Cancer J Clin*. 2021;71(3):209–49.
2. Small W Jr, Bacon MA, Bajaj A, Chuang LT, Fisher BJ, Harkenrider MM, Jhingran A, Kitchener HC, Mileskin LR, Viswanathan AN, et al. Cervical cancer: a global health crisis. *Cancer*. 2017;123(13):2404–12.
3. Datta NR, Stutz E, Liu M, Rogers S, Klingbiel D, Siebenhüner A, Singh S, Bodis S. Concurrent chemoradiotherapy vs. radiotherapy alone in locally advanced cervix cancer: a systematic review and meta-analysis. *Gynecol Oncol*. 2017;145(2):374–85.
4. Huang Z, Mayr NA, Yuh WT, Lo SS, Montebello JF, Grecula JC, Lu L, Li K, Zhang H, Gupta N, et al. Predicting outcomes in cervical cancer: a kinetic model of tumor regression during radiation therapy. *Cancer Res*. 2010;70(2):463–70.
5. Zhang H, Wang X, Ma Y, Zhang Q, Liu R, Luo H, Wang Z. Review of possible mechanisms of radiotherapy resistance in cervical cancer. *Front Oncol* 2023, 13.
6. Qian XB, Chen T, Xu YP, Chen L, Sun FX, Lu MP, Liu YX. A guide to human microbiome research: study design, sample collection, and bioinformatics analysis. *Chin Med J (Engl)*. 2020;133(15):1844–55.
7. Nejman D, Liviyan I, Fuks G, Gavert N, Zwang Y, Geller LT, Rotter-Maskowitz A, Weiser R, Mallel G, Gigi E, et al. The human tumor microbiome is composed of tumor type-specific intracellular bacteria. *Science*. 2020;368(6494):973–80.
8. Fu A, Yao B, Dong T, Chen Y, Yao J, Liu Y, Li H, Bai H, Liu X, Zhang Y, et al. Tumor-resident intracellular microbiota promotes metastatic colonization in breast cancer. *Cell*. 2022;185(8):1356–e13721326.
9. Helmink BA, Khan MAW, Hermann A, Gopalakrishnan V, Wargo JA. The microbiome, cancer, and cancer therapy. *Nat Med*. 2019;25(3):377–88.
10. Riquelme E, Zhang Y, Zhang L, Montiel M, Zoltan M, Dong W, Quesada P, Sahin I, Chandra V, San Lucas A, et al. Tumor Microbiome Diversity and Composition Influence Pancreatic Cancer outcomes. *Cell*. 2019;178(4):795–e806712.
11. Li Z, Zhang Y, Hong W, Wang B, Chen Y, Yang P, Zhou J, Fan J, Zeng Z, Du S. Gut microbiota modulate radiotherapy-associated antitumor immune responses against hepatocellular carcinoma Via STING signaling. *Gut Microbes*. 2022;14(1):2119055.
12. Sasaki T, Matsumoto Y, Murakami K, Endo S, Toyozumi T, Otsuka R, Kinoshita K, Hu J, Iida S, Morishita H et al. Gut microbiome can predict chemoradiotherapy efficacy in patients with esophageal squamous cell carcinoma. *Esophagus* 2023.
13. Dong J, Li Y, Xiao H, Zhang S, Wang B, Wang H, Li Y, Fan S, Cui M. Oral microbiota affects the efficacy and prognosis of radiotherapy for colorectal cancer in mouse models. *Cell Rep*. 2021;37(4):109886.
14. Huang X, Li C, Li F, Zhao J, Wan X, Wang K. Cervicovaginal microbiota composition correlates with the acquisition of high-risk human papillomavirus types. *Int J Cancer*. 2018;143(3):621–34.
15. Rosário A, Sousa A, Varandas T, Marinho-Dias J, Medeiros R, Martins G, Monteiro P, Sousa H. Impact of cervicovaginal microbiome on the risk of cervical abnormalities development. *J Med Virol*. 2023;95(5):e28762.
16. Watanabe Y, Nakamura S, Ichikawa Y, Ii N, Kawamura T, Kondo E, Ikeda T, Nomoto Y, Sakuma H. Early alteration in apparent diffusion coefficient and tumor volume in cervical cancer treated with chemoradiotherapy or radiotherapy: incremental prognostic value over pretreatment assessments. *Radiother Oncol*. 2021;155:3–9.
17. Zhong W, Wu K, Long Z, Zhou X, Zhong C, Wang S, Lai H, Guo Y, Lv D, Lu J, et al. Gut dysbiosis promotes prostate cancer progression and docetaxel resistance via activating NF-kappaB-IL6-STAT3 axis. *Microbiome*. 2022;10(1):94.
18. Chen S, Zhou Y, Chen Y, Gu J. Fastp: an ultra-fast all-in-one FASTQ preprocessor. *Bioinformatics*. 2018;34(17):i884–90.
19. Magoč T, Salzberg SL. FLASH: fast length adjustment of short reads to improve genome assemblies. *Bioinformatics*. 2011;27(21):2957–63.
20. Bokulich NA, Subramanian S, Faith JJ, Gevers D, Gordon JI, Knight R, Mills DA, Caporaso JG. Quality-filtering vastly improves diversity estimates from Illumina amplicon sequencing. *Nat Methods*. 2013;10(1):57–9.
21. Edgar RC. UPARSE: highly accurate OTU sequences from microbial amplicon reads. *Nat Methods*. 2013;10(10):996–8.
22. Edgar RC, Haas BJ, Clemente JC, Quince C, Knight R. UCHIME improves sensitivity and speed of chimera detection. *Bioinformatics*. 2011;27(16):2194–200.
23. Wang Q, Garrity GM, Tiedje JM, Cole JR. Naïve bayesian classifier for Rapid assignment of rRNA sequences into the New Bacterial Taxonomy. *Appl Environ Microbiol*. 2007;73(16):5261–7.
24. Pruesse E, Quast C, Knittel K, Fuchs BM, Ludwig W, Peplies J, Glöckner FO. SILVA: a comprehensive online resource for quality checked and aligned ribosomal RNA sequence data compatible with ARB. *Nucleic Acids Res*. 2007;35(21):7188–96.
25. Altschul SF, Gish W, Miller W, Myers EW, Lipman DJ. Basic local alignment search tool. *J Mol Biol*. 1990;215(3):403–10.
26. Liu M, Li Q, Tan L, Wang L, Wu F, Li L, Zhang G. Host-microbiota interactions play a crucial role in oyster adaptation to rising seawater temperature in summer. *Environ Res*. 2023;216(Pt 2):114585.

27. Lin D, El Alam MB, Jaoude JA, Kouzy R, Phan JL, Elnaggar JH, Resendiz B, Medrano AYD, Lynn EJ, Nguyen ND, et al. Microbiome Dynamics during Chemoradiation Therapy for Anal Cancer. *Int J Radiat Oncol Biol Phys*. 2022;113(5):974–84.
28. Caporaso JG, Kuczynski J, Stombaugh J, Bittinger K, Bushman FD, Costello EK, Fierer N, Peña AG, Goodrich JK, Gordon JI, et al. QIIME allows analysis of high-throughput community sequencing data. *Nat Methods*. 2010;7(5):335–6.
29. Segata N, Izard J, Waldron L, Gevers D, Miropolsky L, Garrett WS, Huttenhower C. Metagenomic biomarker discovery and explanation. *Genome Biol*. 2011;12(6):R60.
30. Camp RL, Dolled-Filhart M, Rimm DL. X-tile: a new bio-informatics tool for biomarker assessment and outcome-based cut-point optimization. *Clin Cancer Res*. 2004;10(21):7252–9.
31. Lu Y-Q, Qiao H, Tan X-R, Liu N. Broadening oncological boundaries: the intratumoral microbiota. *Trends Microbiol*. 2024;32(8):807–22.
32. Singleton DC, Macann A, Wilson WR. Therapeutic targeting of the hypoxic tumour microenvironment. *Nat Reviews Clin Oncol*. 2021;18(12):751–72.
33. Zhen W, Weichselbaum RR, Lin W. Nanoparticle-mediated Radiotherapy remodels the Tumor Microenvironment to Enhance Antitumor Efficacy. *Adv Mater* 2023, 35(21).
34. Hanahan D. Hallmarks of Cancer: New dimensions. *Cancer Discov*. 2022;12(1):31–46.
35. Sun L, Ke X, Guan A, Jin B, Qu J, Wang Y, Xu X, Li C, Sun H, Xu H et al. Intratumoral microbiome can predict the prognosis of hepatocellular carcinoma after surgery. *Clin Translational Med* 2023, 13(7).
36. Zhang M, Zhang Y, Sun Y, Wang S, Liang H, Han Y, Abdulhay E. Intratumoral Microbiota impacts the first-line treatment efficacy and survival in Non-small Cell Lung Cancer patients Free of Lung infection. *J Healthc Eng*. 2022;2022:1–7.
37. Abdolalipour E, Mahooti M, Salehzadeh A, Torabi A, Mohebbi SR, Gorji A, Ghaemi A. Evaluation of the antitumor immune responses of probiotic *Bifidobacterium bifidum* in human papillomavirus-induced tumor model. *Microb Pathog*. 2020;145:104207.
38. Sivan A, Corrales L, Hubert N, Williams JB, Aquino-Michaels K, Earley ZM, Benyamini FW, Lei YM, Jabri B, Alegre ML, et al. Commensal *Bifidobacterium* promotes antitumor immunity and facilitates anti-PD-L1 efficacy. *Science*. 2015;350(6264):1084–9.
39. Cha M-K, Lee D-K, An H-M, Lee S-W, Shin S-H, Kwon J-H, Kim K-J, Ha N-J. Antiviral activity of *Bifidobacterium adolescentis* SPM1005-A on human papillomavirus type 16. *BMC Med*. 2012;10(1):72.
40. Chao X, Wang L, Wang S, Lang J, Tan X, Fan Q, Shi H. Research of the potential vaginal microbiome biomarkers for high-Grade squamous intraepithelial lesion. *Front Med* 2021, 8.
41. Curty G, Costa RL, Siqueira JD, Meyrelles AI, Machado ES, Soares EA, Soares MA. Analysis of the cervical microbiome and potential biomarkers from postpartum HIV-positive women displaying cervical intraepithelial lesions. *Sci Rep* 2017, 7(1).
42. Gilbert JA, Lynch SV. Community ecology as a framework for human microbiome research. *Nat Med*. 2019;25(6):884–9.
43. Wang Z, Xiao R, Huang J, Qin X, Hu D, Guo E, Liu C, Lu F, You L, Sun C, et al. The diversity of Vaginal Microbiota predicts Neoadjuvant Chemotherapy responsiveness in locally Advanced Cervical Cancer. *Microb Ecol*. 2021;84(1):302–13.
44. Mitra A, MacIntyre DA, Marchesi JR, Lee YS, Bennett PR, Kyrgiou M. The vaginal microbiota, human papillomavirus infection and cervical intraepithelial neoplasia: what do we know and where are we going next? *Microbiome*. 2016;4(1):58.
45. Mitra A, MacIntyre DA, Lee YS, Smith A, Marchesi JR, Lehne B, Bhatia R, Lyons D, Paraskevaidis E, Li JV, et al. Cervical intraepithelial neoplasia disease progression is associated with increased vaginal microbiome diversity. *Sci Rep*. 2015;5:16865.
46. Zeber-Lubecka N, Kulecka M, Lindner B, Krynicki R, Paziewska A, Nowakowski A, Bidzinski M, Ostrowski J. Increased diversity of a cervical microbiome associates with cervical cancer. *Front Oncol* 2022, 12.
47. Pushalkar S, Hundeyin M, Daley D, Zambirinis CP, Kurz E, Mishra A, Mohan N, Aykut B, Usyk M, Torres LE, et al. The pancreatic Cancer Microbiome promotes oncogenesis by induction of Innate and Adaptive Immune suppression. *Cancer Discov*. 2018;8(4):403–16.
48. Cieplak T, Soffer N, Sulakvelidze A, Nielsen DS. A bacteriophage cocktail targeting *Escherichia coli* reduces *E. coli* simulated gut conditions, while preserving a non-targeted representative commensal normal microbiota. *Gut Microbes* 2018:1–9.
49. Dolgin E. Fighting cancer with microbes. *Nature*. 2020;577(7792):S16–8.
50. Lenis AT, Lec PM, Chamie K. Bladder Cancer. *JAMA*. 2020;324(19):2006.
51. Twumasi-Boateng K, Pettigrew JL, Kwok YYE, Bell JC, Nelson BH. Oncolytic viruses as engineering platforms for combination immunotherapy. *Nat Rev Cancer*. 2018;18(7):419–32.
52. Bommareddy PK, Shettigar M, Kaufman HL. Integrating oncolytic viruses in combination cancer immunotherapy. *Nat Rev Immunol*. 2018;18(8):498–513.
53. Harrington K, Freeman DJ, Kelly B, Harper J, Soria JC. Optimizing oncolytic virotherapy in cancer treatment. *Nat Rev Drug Discovery*. 2019;18(9):689–706.
54. Wang W, Zheng Y, Wu Z, Wu M, Chen Y, Zhang Y, Fu S, Wu J. Antibody targeting of anaerobic bacteria warms cold tumors and improves the abscopal effect of radiotherapy. *J Translational Med* 2024, 22(1).
55. de Cena JA, Zhang J, Deng D, Dame-Teixeira N, Do T. Low-abundant microorganisms: the Human Microbiome's Dark Matter, a scoping review. *Front Cell Infect Microbiol*. 2021;11:689197.

Publisher's note

Springer Nature remains neutral with regard to jurisdictional claims in published maps and institutional affiliations.